Medicinal Chemistry Research (2019) 28:1235–1245
https://doi.org/10.1007/s00044-019-02368-8

MEDICINAL CHEMISTRY RESEARCH

ORIGINAL RESEARCH

Pyrazole–chalcone derivatives as selective COX-2 inhibitors: design, virtual screening, and in vitro analysis

Anelise F. Macarini[1,2] · Thales U. C. Sobrinho[3] · Gerusa W. Rizzi[1] · Rogério Corrêa[1,2,3]

Received: 26 February 2019 / Accepted: 21 May 2019 / Published online: 30 May 2019

Abstract

In the process of research and development of new drugs, in silico analyzes are widely used. They address the pharmacokinetics of the molecules in study and can predict the binding mode and affinity, using a docking software. This approach can optimize the development of new drugs, reducing costs, time, and resources. In this study, a library of 300 pyrazole–chalcone derivatives were designed, the in silico ADMET (absorption, distribution, metabolism, excretion, and toxicity) properties were evaluated, and a structure-based virtual screening was performed using AutoDock Vina. The docking results exhibited that the derivatives binding mode at the COX-2 active site is similar to celecoxib, the reference drug, and presented similar binding energy. Six compounds were synthetized and tested for in vitro inhibition of the COX-1 and COX-2 isoenzymes and the selectivity index (SI) was calculated. The compound 2a11 showed the best activity for COX-2 (IC_{50}COX-2 = 0.73 μM) whereas the control, celecoxib, resulted IC_{50}COX-2 = 0.88 μM. All the other compounds synthetized presented better potency for COX-2 inhibition than the control. Compound 2a23 exhibited the higher SI, of 280.17 (IC_{50}COX-1 = 210.13 μM/ IC_{50}COX-2 = 0.75 μM), while celecoxib was 246.88 (IC_{50}COX-1 = 217.26 μM/ IC_{50}COX-2 = 0.88 μM). These results corroborate with a possible anti-inflammatory activity and COX-2 selectivity of the new compounds synthetized.

Keywords Pyrazole-Chalcones · Molecular docking · Medicinal Chemistry · COX-2 inhibition · ADMET · Anti-inflammatory

Introduction

Inflammation is an organism response to tissue rupture and, also, initiate the reparation and cure process (Serhan and Savill 2005; Sugimoto et al. 2016). The problem is when this process stop being functional, and prolongate, becoming a chronic inflammation. This can lead to irreversible tissue damages and function loss. The nonsteroidal anti-inflammatory drugs (NSAIDs) are the most used drugs to combat inflammation having this effect due to inhibition of the ciclooxigenases (COXs) (Khalaf et al. 2018; Umamaheswaran et al. 2018). The main problem of NSAIDs use is the gastrointestinal adverse effects, caused by unselective COX inhibition (Rayar et al. 2017). There are two main COX enzymes, COX-1, which is constitutive and participate in physiologic processes, and COX-2, that is induced in inflammatory processes (Umamaheswaran et al. 2018). Due to the adverse effects caused by unselective COX inhibition, selective COX-2 inhibitors, the coxibes, were introduced in the therapeutics (Rayar et al. 2017; Schmidt et al. 2016). This decreased the gastrointestinal problems, but, the coxibes presented severe cardiovascular side effects (Hawkey 1999; Patrono and Baigent 2017; Schmidt et al. 2016). Thus, new drug development is necessary to diminish these side effects.

Drug development is an expensive process and reducing fails, as early as possible, is the main goal of the researchers and the pharmaceutical industry (Egan et al. 2000; van de Waterbeemd and Gifford 2003). In silico predictions can aid

✉ Rogério Corrêa
roger@univali.br

[1] Núcleo de Investigações Químico-Farmacêuticas/NIQFAR, UNIVALI, Rua Uruguai, 458, Itajai, Santa Catarina 88302-901, Brasil

[2] Programa de Pós-Graduação em Ciências Farmacêuticas, Universidade do Vale do Itajaí—UNIVALI, Rua Uruguai, 458, Itajai, Santa Catarina 88302-901, Brasil

[3] Curso de Engenharia Química, Escola do Mar, Ciência e Tecnologia, UNIVALI, Rua Uruguai, 458, Itajai, Santa Catarina 88302-901, Brasil

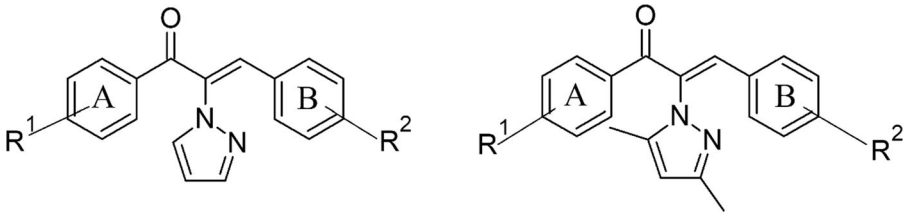

Fig. 1 Series 1 (left) and 2 (right) of the designed compounds, where R^1 is the Topliss substituents, and R^2 is 30 different possible bioactive substituents

in this process by reducing the number of molecules synthetized and tested, once many of the molecule properties can be calculated beforehand. Tools and models available can predict absorption, distribution, metabolism, excretion, and toxicity (ADMET) properties, and structure-based in silico tools, as molecular docking, can predict the possible interactions with the target of study (Danielson et al. 2017).

ADMET tools sometimes use filters based on rules, as the "Rule of five" introduced by Lipinski (Lipinski 2016; Lipinski et al. 1997), and other filters that followed (Egan et al. 2000; Ghose et al. 1999; Martin 2005; Muegge et al. 2001; Teague et al. 1999; Veber et al. 2002) that attempt to predict oral passive absorption and bioavailability. In addition to these, inhibition of metabolism enzymes are important to evaluate metabolic conditions and identification of molecules or fragments potentially toxic or problematics (Baell and Holloway 2010; Brenk et al. 2008). Another approach is the structure-based virtual screening, using molecular docking programs, like AutoDock Vina (Trott and Olson 2009). These programs can predict the binding energy of the ligand–protein complex. AutoDock Vina employs an iterated local search global optimizer, and, among other tested programs, achieved one of the best scoring powers (Wang et al. 2016), which substantiate its use for Virtual Screening.

Bioactive small molecules tested in these analyses are sometimes derived of natural products, as chalcones. In nature, chalcones are precursors in the biosynthesis of flavonoids, and can be isolated from superior plants (Gaonkar and Vignesh 2017; Gomes et al. 2017; Singh et al. 2014). In organic synthesis, there are several methods for the preparation of chalcones, the most known is the Claisen–Schmidt condensation. Chemically these compounds have two aromatic rings that are linked by an aliphatic three-carbon chain composed by an α,β-unsaturated ketone (Gaonkar and Vignesh 2017; Singh et al. 2014). In terms of biological activity, they are reportedly to have anti-inflammatory activity, as well as COX-2 selectivity (Bandgar et al. 2010; Li et al. 2017; Singh et al. 2014; Zhuang et al. 2017). Pyrazole derivatives are other example of small molecules that are largely studied (Karrouchi et al. 2018; Khan et al. 2016; Li and Zhao 2014), including for its anti-inflammatory activity (Mukarram et al. 2017; Viveka et al. 2018) and the specific interaction with COX-2 (Shen et al. 2017).

Chalcone variation can be made using three main strategies. They are: structural modification in the aryl rings, substitution of one or both aryl rings by heteroaryl rings, and, molecular hybridization through conjugation with biologically active molecules (Özdemir et al. 2017). This work contemplates the use the first and third strategy to evaluate the activity of pyrazole–chalcone derivatives as COX-2 inhibitors.

Material and methods

Design and in silico analysis

The pyrazole–chalcone derivatives were designed based in the conjugation of a chalcone and a pyrazole nucleus, linked on the aliphatic instauration, forming the backbone of the molecules. As shown in Fig. 1 ring A of the chalcone moiety was modified using the classical Topliss substituents (Richter 2017; Topliss 1972). Ring B was modified using 30 different possible bioactive substituents. Also, the pyrazole ring was derived using, as starting materials, the unsubstituted pyrazole ring, and the 3,5-dimethylpyrazole. This resulted in two series of 150 compounds each. The molecules were drawn with ACD/ChemSketch 2017.2.1 (ACD/Labs) freeware.

ADMET analysis

The online free tool SwissADME (swissadme.ch) (Daina et al. 2017) was used to calculate physicochemical properties, lipophilicity, water solubility, pharmacokinetics, druglikeness, and other chemometrics or medicinal chemistry parameters.

Docking

The molecular docking was performed using AutoDock Vina (Trott and Olson 2009). The ligands were assumed to be flexible and the protein, rigid. The ligand setup was of six poses maximum with exhaustiveness of 14, being selected and presented the ones with better energy of binding. The protein was obtained from Protein Data Bank (PDB) (Berman 2000), code 3LN1 (Wang et al. 2010), and, was prepared in Chimera 2.1 (Pettersen et al. 2004) as

follow: chain A was isolated, charges and polar hydrogens added, and the solvent removed. The ligands were prepared using AutoDock Tools (Morris et al. 2009). The root mean square deviation (RMSD) was calculated between the crystallography celecoxib pose and the docked pose. If RMSD < 2 Å, the docking was accepted as valid.

After the docking procedures, the poses were visualized in Chimera 2.1, H-bonds and other non-covalent interactions were accounted for and pictures saved. BIOVIA Discovery Studio 2017 was used to produce the 2D diagram of the docked poses.

Synthesis

All reagents were purchased from Vetec® and Sigma–Aldrich® and were analytic grade. All reactions were monitored using thin layer chromatography (TLC), Macherey–Nagel® pre-coated aluminium sheets 0.2 mm silica gel with fluorescent indicator UV_{254}, (eluent hexane: ethyl acetate, 80:20). The synthesis was performed in three steps, as follows.

Final products characterization was done by Infrared (FT-IR), recorded with an IR-Prestige—21 (Shimadzu Inc. —Tokyo, Japan); ^{1}H and ^{13}C NMR, that were recorded on a Bruker ADVANCE DPT-300 (Bruker, Karlsruhe, Germany); and elemental analysis that were performed in a Perkin Elmer 2400 Series II CHNS/O System—Elemental Analyzer (Perkin Elmer—Massachusetts, USA), operating in three modes: CHN, CHNS, and Oxygen, in the range of temperature from 100 to 1100 °C.

Phenacyl bromide synthesis

Substituted acetophenones (4-H, 4-Cl and 4-OCH_3), 2 mmol, were dissolved in acetic acid. Pyridinium tribromide (2 mmol) was added to the solution. The reaction occurred in microwave reactor (CEM Discovery) for 30 min at 80 °C under reflux. After the completion of the reaction, cold water was added to the mixture and stirred until complete precipitation. The precipitate was filtered and dried in vacuum desiccator with silica gel as drying agent. No purification was needed.

2-bromo-1-phenylethan-1-one (1a) Yield 67%; mp 50 °C. ^{1}H NMR ($CDCl_3$, 300 MHz) δ = 5.49 (2H, s, H-9a, b); 7.48–7.53 (2H, t, J = 7.2 Hz, H-3, 5); 7.60–7.63 (1H, t, H- J = 7.2 Hz, H-1); 7.97–7.99 (2H, d, J = 7.2Hz H-2, 6).

2-bromo-1-(4-methoxyphenyl)ethan-1-one (1c) Yield 54%; mp 72 °C. ^{1}H NMR ($CDCl_3$, 300 MHz) δ = 5,41 (2H, s, H-11a, b); 3.78 (3H, s, H-11a, b, c); 7.44–7.47 (2H, d, J = 8.5 Hz, H-3, 5); 7.82–7.85 (2H, d, H- J = 8.5 Hz, H-2, 6).

2-bromo-1-(4-chlorophenyl)ethan-1-one (1d) Yield 70%; mp 96 °C. ^{1}H NMR ($CDCl_3$, 300 MHz) δ = 5.44 (2H, s, H-10a, b); 7.46–7.49 (2H, d, J = 8.7 Hz, H-3, 5); 7.90–7.93 (2H, d, J = 8.7 Hz, H-2, 6).

2-(3,05-dimethyl-1H-pyrazol-01-yl)-01-phenylethan-01-one intermediates synthesis

One millimolar of 3,5-dimethylpyrazole was dissolved in acetonitrile, and, K_2CO_3 (2eq.) was added. One millimolar of the wanted substituted phenacyl bromide (1a, 1c, and 1d) was added to the mixture. The reaction was assisted by a microwave reactor (CEM Discovery) for 60 min at 82 °C under reflux. After the completion of the reaction, cold water was added to the mixture and stirred until complete precipitation. The precipitate was filtered off and dried overnight in vacuum desiccator with silica gel as drying agent. The product was recrystallized with cyclohexane.

2-(3,5-dimethyl-1H-pyrazol-1-yl)-1-phenylethan-1-one (2a) Yield 67%; mp 95 °C. ^{1}H NMR ($CDCl_3$, 300 MHz) δ = 2.16 (3H, s, H-9a, b, c); 2.24 (3H, s, H-10a, b, c); 5.46 (2H, s, H-6a, b); 5.91 (1H, s, H-4); 7.48–7.53 (2H, t, J = 7.2 Hz, H-13,15); 7.60–7.63 (1H, t, J = 7.2 Hz, H-14); 7.97–7.99 (2H, d, J = 7.2Hz H-12, 16).

2-(3,5-dimethyl-1H-pyrazol-1-yl)-1-(4-methoxyphenyl) ethan-1-one (2c) Yield 54%; mp 104 °C. ^{1}H NMR ($CDCl_3$, 300 MHz) δ = 2.14 (3H, s, H-9a, b, c); 2.21 (3H, s, H-10a, b, c); 3.74 (3H, s, H-18a, b, c); 5.39 (2H, s, H-6a, b); 5.88 (1H, s, H-4); 7.44–7.47 (2H, d, J = 8.5 Hz, H-13, 15); 7.82–7.85 (2H, d, J = 8.5 Hz, H-12, 16).

1-(4-chlorophenyl)-2-(3,5-dimethyl-1H-pyrazol-1-yl)ethan-1-one (2d) Yield 70%; mp 155 °C. ^{1}H NMR ($CDCl_3$, 300 MHz) δ = 2.16 (3H, s, H-9a, b, c); 2.23 (3H, s, H-10a, b, c); 5.40 (2H, s, H-6a, b); 5.90 (1H, s, H-4); 7.46–7.49 (2H, d, J = 8.4 Hz, H-13, 15); 7.90–7.93 (2H, d, J = 8.4 Hz, H-12, 16).

4-[(1Z)-2-(3,5-dimethyl-1H-pyrazol-1-yl)-3-oxo-3-phenylprop-1-en-1-yl]benzonitrile synthesis

0.5 mmol of the respective intermediate (2a, 2c, and 2d) was dissolved in ethanol, and an aqueous solution of K_2CO_3 (2eq.) was added. The substituted benzaldehyde (0.5 mmol) was added to the mixture and it was kept stirring at room temperature for 10 h. After the completion of the reaction, cold water was added to the mixture and stirred until complete precipitation. The precipitate was filtered and dried in vacuum desiccator with silica gel as drying agent. The product was recrystallized with cyclohexane.

4-[(1Z)-2-(3,5-dimethyl-1H-pyrazol-1-yl)-3-oxo-3-phenylprop-1-en-1-yl]benzonitrile (2a11) Yield: 27%; mp 120 °C. IR (KBr cm^{-1}): 1274 (C—N); 1319 (C—N); 1666 (C=O); 2224 (Ar—C≡N). ^{1}H NMR ($CDCl_3$, 300 MHz) δ = 1.92 (3H, s, 9-Ha, b, c); 2.27 (3H, s, H-10a, b, c); 5.98 (1H, s, H-4), 6.98–7.01 (2H, d, J = 8.4 Hz, H-13, 17); 7.41–7.48 (3H, m, J = 7.2 Hz, H-22, 20, H-11); 7.54–7.57 (3H, t, J = 8.4 Hz, H-14, 16); 7.75–7.77 (2H, d, J = 7.5 Hz, H19, 23). ^{13}C NMR ($CDCl_3$, 75.47 MHz) δ = 11.03 (C-10); 13.67 (C-9); 107.36 (C-4); 118.22 (C-24); 133.56 (C-11); 128.57–136.98 (Ar-C); 137.39 (C-6); 140.67 (C-5); 151.04 (C-3); 191.48 (C-7). Anal. calcd. for $C_{21}H_{17}N_3O$ (in %): C-77.04, H-5.23, N-12.84, O-4,89. Found C-77.06, H-5.2, N-12.84, O-4,89.

(2Z)-2-(3,5-dimethyl-1H-pyrazol-1-yl)-3-(4-nitrophenyl)-1-phenylprop-2-en-1-one (2a17) Yield: 31%; mp: 118 °C. IR (KBr cm^{-1}): 1267 (C—N); 1313 (C—N); 1342 (N—O); 1514 (N—O); 1668(C=O). ^{1}H NMR ($CDCl_3$, 300 MHz) δ = 1,93 (3H, s, 9-Ha, b, c); 2.28 (3H, s, H-10a, b, c); 5.99 (1H, s, H-4), 7.06–7.09 (2H, d, J = 8.7 Hz, H- 13, 17); 7.42–7.47 (2H, t, J = 7.5 Hz, H-22, 20); 7.52 (1H, s, H-1); 7.55–7.58 (1H, t, J = 7.5 Hz, H-21); 7.76–7.77 (2H, d, J = 7.5 Hz, H19, 23); 8.11–8.14 (2H, d, J = 9 Hz, H-14, 16). ^{13}C NMR ($CDCl_3$, 75.47 MHz) δ = 11.05 (C-10); 13.65 (C-9); 107.49 (C-4); 123.78 (C-11); 128.61–137.33 (Ar-C); 138.58 (C-6); 140.75 (C-5); 148.25 (C-15); 151.13 (C-3); 191.38 (C-7). Anal. calcd. for $C_{20}H_{17}N_3O_3$ (in %): C-69.15, H-4.93, N-12.1, O-13.82. Found C-69.16, H-4.9, N-12.1, O-13.83.

N-{4-[(1Z)-2-(3,5-dimethyl-1H-pyrazol-1-yl)-3-oxo-3-phenylprop-1-en-1-yl]phenyl}acetamide (2a23) Yield: 30%; mp: 187 °C. IR (KBr cm^{-1}): 1321 (C—N); 1373 (C—N); 1660 (C=O); 1674(C=O); 3319 (N—H). ^{1}H NMR ($CDCl_3$, 300 MHz) δ = 1.96 (3H, s, H-27a, b, c); 2.11 (3H, s, H-9a, b, c); 2.31 (3H, s, H-10a, b, c); 6.01 (1H, s, H-4), 6.73–6.86 (d, 2H, J = 8.7 Hz, H-13, 17); 7.34–7.37 (2H, d, J = 8.4 Hz, H-19, 23); 7.41–7.46 (2H, t, J = 7.2 Hz, H-20, 22); 7.49 (1H, s, H-11); 7.53–7.55 (1H, t, J = 7.2 Hz, H-21); 7.71–7.74 (2H, d, J = 6.9 Hz, H-14, 16); 8.08 (1H, s, NH-24). ^{13}C NMR ($CDCl_3$, 75.47 MHz) δ = 10.92 (C-10); 13.77 (C-9); 24.60 (C-27); 106.74 (C-4); 119.43 (C-11); 127.44–133.22 (C-Ar); 137.46 (C-6); 140.93 (5-C); 150.33 (C-3); 168.67 (C-25); 192.34 (C-7). Anal. calcd. for $C_{22}H_{21}N_3O_2$ (in %): C-73.52, H-5.89, N-11.69, O-8.9. Found C-73.53, H-5.85, N-11.7, O-8.91.

(2Z)-3-(4-chlorophenyl)-2-(3,5-dimethyl-1H-pyrazol-1-yl)-1-phenylprop-2-en-1-one (2a7) Yield: 35%; mp: 147 °C. IR (KBr cm^{-1}): 1089 (Ar—Cl); 1273 (C—N); 1317 (C—N); 1658 (C=O). ^{1}H NMR ($CDCl_3$, 300 MHz) δ = 1.93 (3H, s, H-9a, b, c); 2.29 (3H, s, H-10a, b, c); 5.98 (1H, s, H-4), 6.79–6.82 (2H, d, J = 8.7 Hz, H-13, 17); 7.23–7.26 (2H,d, J = 7.8 Hz, H-19, 23); 7.41–7.46 (2H, t, J = 7.5 Hz, H-20, 22); 7.49 (1H, s, H-11); 7.53–7.55 (1H, t, J = 7.2 Hz, H-21); 7.75–7.77 (2H, d, J = 7.5 Hz, H-14, 16). ^{13}C NMR ($CDCl_3$, 75.47 MHz) δ = 10.94 (C-10); 13.73 (C-9); 106.89 (C-4); 128.45 (C-11); 129.14–137.10 (C-Ar); 139.74 (C-6); 140.66 (C-5); 150.61 (C-3); 191.98 (C-7). Anal. calcd. for $C_{20}H_{17}ClN_2O$ (in %): C-71.32, H-5.09, N-8.32, O-4.75. Found C-71.32, H-5.05, N-8.32, O-4.76.

(2Z)-3-(4-chlorophenyl)-2-(3,5-dimethyl-1H-pyrazol-1-yl)-1-(4-methoxyphenyl)prop-2-en-1-one (2c7) Yield: 15%; mp: 151 °C. IR (KBr cm^{-1}): 1089 (Ar—Cl); 1112 (C—O—C); 1271 (C—N); 1322 (C—N); 1689 (C=O). ^{1}H NMR (Acetone-d_6, 300 MHz) δ = 1.95 (3H, s, H-9a, b, c); 2.79 (3H, s, H-10a, b, c); 3.91 (3H, s, H-26a, b, c); 4.73 (1H, s, H-4), 5.71 (1H, s, H-11); 7.04–7.06 (d, 2H, J = 6.9 Hz, H-13, 17); 7.16–7.18 (2H, d, J = 6.6 Hz, H-19, 23); 7.31–7.33 (2H, d, J = 6.9 Hz, H-20, 22); 8.24–8.26 (2H, d, J = 6.9 Hz, H-14, 16). ^{13}C NMR (Acetone-d_6, 75.47 MHz) δ = 10.10 (C-10); 12.72 (C-9); 55.19 (C-26); 106.17 (C-4); 113.86 (C-11); 128.14–132.59 (C-Ar); 134.50 (C-6); 141.78 (C-5); 149.04 (C-3); 164.57 (C-21); 188.50 (C-7). Anal. calcd. for $C_{21}H_{19}ClN_2O_2$ (in %): C-68.76, H-5.22, N-7.64, O-8.72. Found C-68.76, H-5.18, N-7.64, O-8.73.

4-[(1Z)-3-(4-chlorophenyl)-2-(3,5-dimethyl-1H-pyrazol-1-yl)-3-oxoprop-1-en-1-yl]benzonitrile (2d11) Yield: 29%; mp: 149 °C. IR (KBr cm^{-1}): 1089 (Ar—Cl); 1271 (C—N); 1328 (C—N); 1664 (C=O); 2227 (Ar—C≡N). ^{1}H NMR ($CDCl_3$, 300 MHz) δ = 1.90 (3H, s, H-9a, b, c); 2.27 (3H, s, H-10a, b, c); 5.98 (1H, s, H-4); 6.99–7.02 (2H, d, J = 8.4 Hz, H-13, 17a); 7.41–7.38 (2H, d, J = 8.7 Hz, H-19, 23); 7.49 (1H, s, H-11); 7.55–7.58 (2H, d, J = 8.4 Hz, H-20, 22); 7.65–7.68 (2H, d, J = 8.4 Hz, H-14, 16). ^{13}C NMR ($CDCl_3$, 75.47 MHz) δ = 10.47 (C-10); 13.34 (C-9); 106.95 (C-4); 119.75 (C-11); 121.24 (C-24); 128.21-134.17 (C-Ar); 138.14 (C-6); 140.54 (C-5); 150.72 (C-3); 191.45 (C-7). Anal. calcd. for $C_{21}H_{16}ClN_3O$ (in %): C-69.71, H-4.46, N-11.61, O-4.42. Found C-69.71, H-4.43, N-11.62, O-4.43.

In vitro COX-1/COX-2 inhibition assay

The COX (ovine) inhibitor screening assay kit (catalog number 560101, Cayman Chemical, Ann Arbor, MI, USA) was used according to the manufacturer's instructions to directly measure prostaglandin ($PGF_{2\alpha}$) produced by $SnCl_2$ reduction of COX-derived prostaglandin H synthase.

In a recipient was added: assay buffer (150 µl), heme (10 µl), COX-1 or COX-2 enzyme solution (10 µl) and samples or the positive control (celecoxib) (10 µl). In the negative control recipient, the inhibitors weren't added. Then the recipient was shaken carefully for 10 s and

incubated at 37 °C for 5 min. Arachidonic acid solution (10 µl) was added to initiate the conversion of arachidonic acid to PGH_2. The recipients were shaken for 10 s and incubated at room temperature for exactly 2 min. The reaction was stopped by adding acid $SnCl_2$ solution, which is used to reduce the PGH_2 produced in the COX reaction to the more stable $PGF_{2\alpha}$.

In a 96-wells plate, where the wells are previously attached with polyclonal anti-IgG, the previous solution (50 µL) was added to the wells together with a PG-acetylcholinesterase (PG-tracer) (50 µL) and a PG monoclonal antibody (50 µL) that attach to the well. The $PGF_{2\alpha}$ or PG-tracer complexes with the PG monoclonal antibody. The amount of PG-tracer that is able to bind to the well will be inversely proportional to the concentration of $PGF_{2\alpha}$ in the well. This solution was incubated for 18 h. Then, the plates were washed, and, Ellman's Reagent (200 µL), which contains the substrate to acetylcholinesterase, was added. This reaction produces color, and the intensity of it was measured at 405 nm using an ELISA Plate Reader. This color represents the amount of PG-tracer bound to the well, which is inversely proportional to the amount of free $PGF_{2\alpha}$ present in the well during the incubation. Prostaglandin standards were used to construct a standard curve. The absorbance was transformed to pg/ml of $PGF_{2\alpha}$ using standard curve computed on excel. To calculate the selectivity index, the ratio the ratio of IC_{50}COX-1/IC_{50}COX-2.

Results and discussion

ADMET properties

ADMET studies were performed, for the 300 compounds designed, using the SwissADME online tool (swissadme.ch). Results are shown in Table 1—we presented only the results of the synthetized compounds (see section 3.3). In the drug development point of view, the compounds have favorable drug properties, predicting a favorable oral absorption. In the filters based on rules applied, compound 2d11 showed 1 violation in the Muegge filter, due to excessive log P value, threshold was $2 \le XLOGP \le 5$. Only in Leadlikeness filter, all compounds showed at least one violation, and compound 2d11 showed two. These violations relate to high log P ($XLOGP \le 3.5$) for all compounds, and molecular weight ($250 \le MW \le 350$) for compound 2d11. However, Tian et al. (2015) state that drug leads have lower molecular weight and are less complex and less lipophilic than market drugs. Also, lipophilicity does not directly relate to the biophysics of ligand–protein complex, being more of an experimental solubility ratio; on the other hand, H-bond donors and acceptors and molecular weight fit well with how ligand binding sites are formed in proteins (Lipinski 2016).

Regarding metabolization predictions, the program analyzes if the molecules are P-glycoprotein (P-gp) substrates. P-gp acts as an active transporter expelling molecules out of the cell, being able to reduce or prevent absorption of drugs and other substances (Moroy et al. 2012). As none of the synthetized molecules resulted "yes" for P-gp substrate, chances are good that the compounds can be absorbed. The program also predicts inhibition of 5 CYP enzymes. The cytochrome P450 (CYP) is the major, and most studied phase I metabolizing enzyme family. CYPs are responsible for metabolism of approximately 75% of all marketed drugs (Moroy et al. 2012). The most important enzyme of the CYP family is the CYP3A4, which alone metabolizes ~50% of all drugs (Moroy et al. 2012). So is plausible to assume that the synthetized compounds don't affect the metabolism of at least half of all drugs, being that none resulted as an inhibitor for this enzyme. Withal, all the compounds are inhibitors of the CYP2C9 enzyme. In the CYP family, CYP2C9 metabolizes celecoxib, diclofenac, ibuprofen, other nonsteroidal anti-inflammatory drugs (NSAIDs) (Daly et al. 2018) and, possibly, the synthetized compounds.

Docking

To the docking method be considered valid, we calculated the RMSD (root mean square deviation) value between the docked and crystallography pose of celecoxib. The docking would be considered valid if RMSD ≤ 2 Å, and we obtained 0.4 Å, so the docking was considered valid. Then, virtual screening was performed for all the 300 molecules designed using the described method. All compounds showed good energy binding values. Attention was taken for the series 2 compounds, as compounds 2a11 and 2a23. The best scored compounds suggest that the 3,5-dimethylpyrazole (series 2) and unsubstituted A ring (2a derivatives) improve binding affinity.

The best scored molecule was 2a11, with a binding energy of −11kcal/mol, whereas the docked celecoxib presented a binding energy of −12.2 kcal/mol. The results were analyzed using BIOVIN Discovery Studio and Chimera 1.12. Figure 2 shows the 2D diagram of the docked pose of compound 2a11, indicating a hydrogen bond between a phenylalanine residue (Phe504) and the benzonitrile group of ring B that stabilize the compound in the selectivity pocket. Also, non-polar interactions stabilize the compound in the active site (Fig. 3).

Figure 4 presents the second-best docked compound, 2a23, with a binding energy of −10.6 kcal/mol in the best docked pose. Three H-bonds can be visualized, in the selectivity pocket there is one between the nitrogen of amide group of B ring and a leucine residue (Leu338) and

Table 1 ADMET properties calculated with the SwissADME online tool, and docking results, showing the six synthetized compounds

Properties	Parameters	Compounds					
		2a11	2a17	2a23	2a7	2c7	2d11
Docking	Binding energy (kcal/mol)	−11	−10.5	−10.6	−10.4	−8.6	−10
Physicochemical Properties	Mol weight (g/mol)	327.38	347.37	359.42	308.76	338.79	361.82
	Rotatable bonds	4	5	6	4	5	4
	H-bond acceptors	3	4	3	2	3	3
	H-bond donors	0	0	1	0	0	0
	TPSA[a] (Å)	58.68	80.71	63.99	34.89	44.12	58.68
Lipophilicity	iLOGP	2.70	2.52	3.15	2.70	3.14	3.71
	XLOGP3	3.96	4.50	4.79	3.96	4.47	5.99
	WLOGP	4.14	4.18	4.04	4.31	4.32	4.80
	MLOGP	1.91	2.04	2.91	1.91	2.74	4.14
	Silicos-IT log P	3.24	2.03	3.89	3.24	3.86	5.52
	Consensus log P	3.10	3.06	3.82	3.10	3.71	5.01
Water Solubility	ESOL Class	MS[b]	MS	MS	MS	MS	PS
	Ali Class	MS	MS	MS	MS	MS	PS
	Silicos-IT class	MS	MS	PS[c]	MS	PS	PS
Pharmacokinetics	GI[d] absorption	High	High	High	High	High	High
	BBB[e] permeant	Yes	No	Yes	Yes	Yes	Yes
	P-gp[f] substrate	No	No	No	No	No	No
	CYP1A2 inhibitor	No	No	Yes	No	Yes	Yes
	CYP2C19 inhibitor	No	Yes	Yes	No	Yes	Yes
	CYP2C9 inhibitor	Yes	Yes	Yes	Yes	Yes	Yes
	CYP2D6 inhibitor	No	No	No	No	No	No
	CYP3A4 inhibitor	No	No	Yes	No	No	No
Druglikeness	Lipinski violations	0	0	0	0	0	0
	Ghose violations	0	0	0	0	0	0
	Veber violations	0	0	0	0	0	0
	Egan violations	0	0	0	0	0	0
	Muegge violations	0	0	0	0	0	1
	Bioavailability Score	0.55	0.55	0.55	0.55	0.55	0.55
Medicinal Chemistry	PAINS[g] alerts	1	0	1	1	0	0
	Brenk alerts	2	3	1	2	1	1
	Leadlikeness violations	1	1	1	1	1	2
	Synthetic accessibility	3.21	3.18	3.31	3.21	2.89	3.13

[a]Total polar surface area
[b]Moderately soluble
[c]Poorly soluble
[d]Gastrointestinal
[e]Blood-brain barrier
[f]P-glycoprotein
[g]Pan Assay Interference Compounds

the oxygen of the amide carbonyl group and an arginine residue (Arg499). Besides these, the oxygen of the carbonyl group of the chalcone moiety exhibit a H-bond with a serine residue (Ser516), that is one interaction celecoxib don't possess, which can provide a higher selectivity and better stability in the active site. Other non-polar interactions can be visualized in Fig. 5.

The docked poses of the compounds synthetized were superimposed and showed in Fig. 6. The compounds occupy the same space, volumetrically, and geometrically, as the reference drug, celecoxib (in blue). This can lead to the conclusion that the compounds possibly have the same activity as celecoxib, due to similar interactions with the biological receptor.

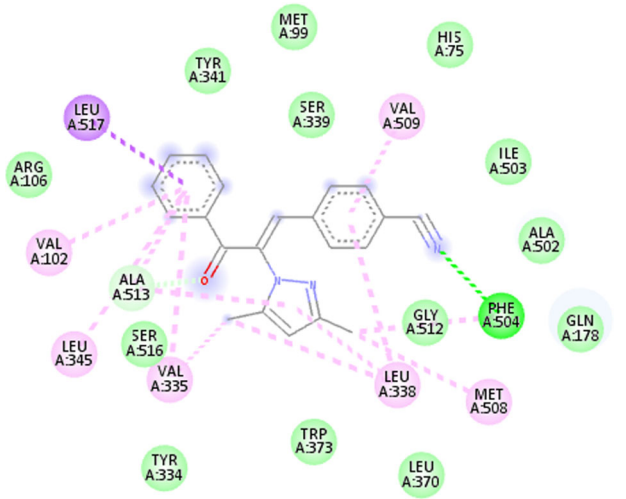

Fig. 2 2D diagram of compound 2a11 in COX-2 active site. Hydrogen bond is shown in green, other interactions, as, van der Waals, pi-sigma, and alkyl, are shown in blue, purple, and pink, respectively

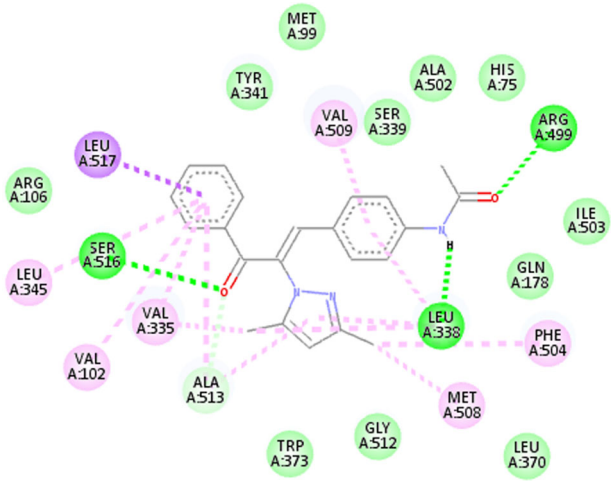

Fig. 4 Docked poses of compound 2a23 in COX-2 active site. Hydrogen bonds are shown in green, other interactions, as, van der Waals, pi-sigma, and alkyl, are shown in blue, purple, and pink, respectively

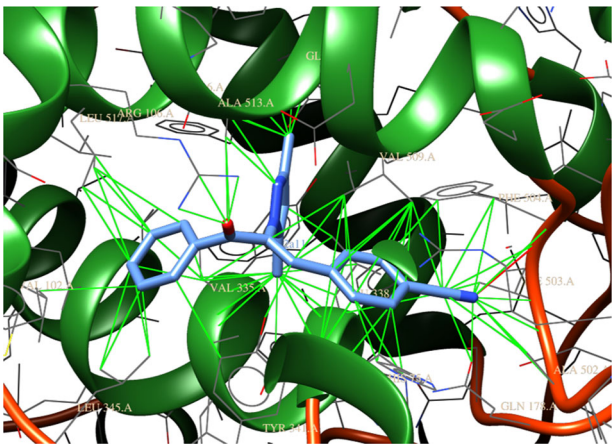

Fig. 3 3D image of compound 2a23 in COX-2 active site. Showing an hydrogen bond in red line, and, other non-polar interactions with the protein in lime green lines

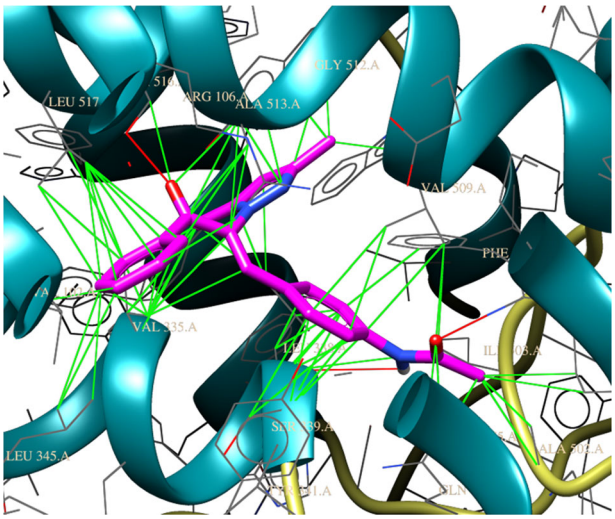

Fig. 5 3D image of compound 2a23 in COX-2 active site. Showing three hydrogen bonds in red lines, and, other non-polar interactions with the protein in lime green lines

Synthesis

From the docking results, six of the 300 molecules designed were synthetized based on the obtained results of binding energy and structure characteristics. To achieve the compounds designed, a three-step synthesis was planned. First, a phenacyl bromide synthesis, then, its reaction with 3,5-dimethylpyrazole, resulting in the 2-(3,5-dimethyl-1*H*-pyrazol-1-yl)-1-phenylethan-1-one intermediates, lastly, the reaction of the intermediates with substituted benzaldehydes, forming the final products 4-[(1*Z*)-2-(3,5-dimethyl-1*H*-pyrazol-1-yl)-3-oxo-3-phenylprop-1-en-1-yl]benzonitrile derivatives as shown in Scheme 1. As is possible to observe, A ring groups come from the acetophenones used to produce the phenacyl bromides, and the B ring groups from the benzaldehydes.

Phenacyl bromides synthesis (1a, 1c, and 1d)

The substituted phenacyl bromides synthesis was done by reaction of the chosen substituted acetophenones with pyridinium tribromide in equimolar amounts, using acetic acid as solvent. All reactions were performed under microwave irradiation. Mean yields of 70% were obtained, without impurities. The melting points found were 50.5, 72.5, and 96.5 °C for the unsubstituted (1a), 4-methoxy (1c) and 4-chloro phenacyl bromide (1d), respectively. In the ^{1}H NMR spectra, it's possible to observe signals of the aromatic ring and a singlet in the 5–6 ppm region respective to the methylene carbon.

2-(3,5-dimethyl-1H-pyrazol-1-yl)-1-phenylethan-1-one intermediates (2a, 2c, and 2d)

The intermediate compounds were synthetized using equimolar amounts of the phenacyl bromides and reacting it with 3,5-dimethylpyrazole, using catalytic amounts of K_2CO_3 and acetonitrile as solvent. The synthesis occurred under microwave irradiation, and the result was a pure product, analyzed by TLC; however, recrystallization with cyclohexane was carried out for the determination of the melting point. The crude yield was 60% and the recrystallized 10%. Characterization was done by ^1H NMR, where was noticeable the appearing of signals referent to the 3,5-dimethylpyrazole ring, e.g., a singlet in 6 ppm referent of the methine carbon, and two singlets in the 2–3ppm region referent of the methoxy groups, in addition to the one present in the phenacyl bromide spectra.

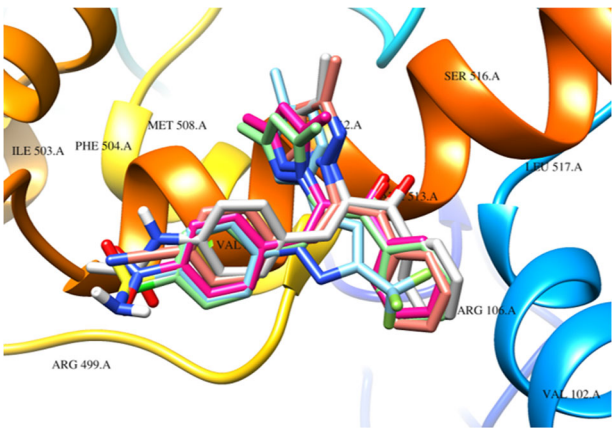

Fig. 6 Docked poses of compounds 2a7, 2a11, 2a17, 2a23, and celecoxib superimposed in the active site of COX-2 enzyme

4-[(1Z)-2-(3,5-dimethyl-1H-pyrazol-1-yl)-3-oxo-3-phenylprop-1-en-1-yl]benzonitrile synthesis (2a7, 2a11, 2a17, 2a23, 2c7, 2d11)

The final product was synthetized using a derivation of the Claisen–Schmidt condensation, once the final products are chalcone derivatives. The intermediate was dissolved in ethanol and catalytic amounts of K_2CO_3 was added to the solution. The chosen benzaldehyde was added, and the reaction occurred at room temperature with constant stirring.

Before choosing the K_2CO_3 as base, we tried the classic strong base, NaOH, but the reaction was too fast, forming too much impurities. The choice of a basic salt, a weaker base, instead of the strong base used in classical Claisen–Schmidt condensation, was due to the reactivity of the methylene carbon in the intermediates (2a, 2c, and 2d).

The chalcone reaction occurs in some steps: first the base, in aqueous solution, attacks the methyl group of acetophenone—in our case the methylene carbon of the intermediates—forming the carbanion. Then, carbanion will attack the carbonyl group of benzaldehyde, followed by a rearrangement and dehydration step, forming the chalcone, and regenerating the base (Enchev and Mehandzhiyski 2017). In the pyrazole ring system, the nitrogen (atom 1) have unshared electrons that conjugates with the aromatic system, and its adjacent nitrogen (atom 2) unshared electrons doesn't (Faria et al. 2017). We suppose that the methylene carbon in our intermediate is more susceptible to the nucleophilic attack by the base, because of the two electronegative groups next to it, which explains why the K_2CO_3 was able to abstract the hydrogen and form the carbanion. However, this carbanion is less reactive than the one formed by the acetophenone, given its more stable. Moreover, presents the steric hindrance factor of the 3,5-

Scheme 1 Synthesis scheme of the pyrazole–chalcone derivatives. **a** (microwave, 80 °C, acetic acid), **b** (microwave, K_2CO_3, acetonitrile), and **c** (room temperature, K_2CO_3, ethanol)

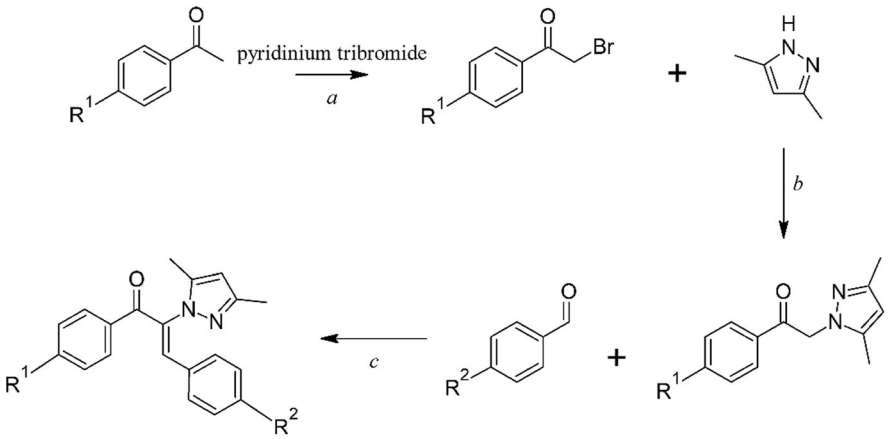

2a11. R^1= H, R^2= CN; **2a17.** R^1= H, R^2= NO_2; **2a23.** R^1= H, R^2= $NHCOCH_3$; **2a7.** R^1= H, R^2= Cl; **2d11.** R^1= Cl, R^2= CN; **2c7.** R^1= OCH_3, R^2= Cl.

Table 2 In vitro enzyme inhibition assay COX-1/COX-2 for synthesized compounds and reference drug (celecoxib)

Compounds	IC_{50} COX-1 (μM)[a]	IC_{50} COX-2 (μM)[a]	IS[b]
2a11	200.64 ± 0.96	0.73 ± 0.02	274.85
2a23	210.13 ± 0.40	0.75 ± 0.04	280.17
2a17	207.76 ± 0.82	0.78 ± 0.02	266.36
2a7	215.48 ± 0.60	0.84 ± 0.004	256.52
2d11	213.40 ± 0.88	0.84 ± 0.006	254.05
2c7	225.86 ± 0.92	0.86 ± 0.002	262.63
Celecoxib	217.72 ± 0.22	0.88 ± 0.002	247.41

All compounds have a $p < 0001$

[a]IC_{50} corresponds to the required concentration of the compound to produce 50% inhibition of COX-1 or COX-2 by three determinations, the mean deviation being less than 10% in all cases. Determined with COX (ovine) Inhibitor Screening Assay Kit (catalog N°. 560101, Cayman Chemicals Inc., Ann Arbor, MI, USA)

[b]IS (selectivity index) IC_{50}COX-1/IC_{50}COX-2

dimethylpyrazole ring, that may difficult the carbanion attack. This can be the reason we obtained lower yields then the normally observed in this reaction.

In vitro COX-1/COX-2 inhibition assay

As shown in Table 2, all the compounds synthesized have lower IC_{50} and better selectivity indexes (SI) than the reference drug (celecoxib) for COX-2 inhibition. It is noted that AutoDock Vina showed a very precise scoring power for the designed and synthetized ligands, since the compound with better binding energy was also the one that presented the lowest IC_{50} for COX-2. It should be stated that celecoxib, used as a control, is the ligand with lowest docking energy, but obtained a less potent IC_{50} then the other tested compounds.

The SI shows the ratio of IC_{50}COX-1/IC_{50}COX-2, where compound 2a23 has the best SI, being greater than the reference drug. These results corroborate the docking analysis, where the compound 2a23 showed interactions with COX-2, outside the selectivity pocket, whereas celecoxib did not. The reason, this compound is less potent for COX-1, may be due to the steric effect caused by the large volume of its substituent on the B ring. The other compounds tested also have higher selectivity indexes than celecoxib.

Besides the anti-inflammatory effects, selectively inhibiting COX-2 can have a protective effect on breast cancer risk, regarding estrogen-responsive cancer (de Pedro et al. 2015). Also, anti-angiogenesis caused by inhibition of COX-2 were presented as an innovative strategy to a synergetic treatment efficacy of hypoxia-responsive prodrugs in cancer treatment (Kim et al. 2018). This reinforce the importance of continuing this study in cell and animal models, evaluating all the biological effects of these compounds and possibly finding a hit molecule and future drug.

Conclusions

In the present study, new potential COX-2 selective inhibitors were designed and analyzed thorough ADMET filters and structure-based virtual screening, using molecular docking. The results showed that the compounds of the series 2, with the 3,5-dimethylpyrazole ring, and that possessed polar groups that can interact through H-bonds with the enzyme in ring A, were the best scored docked molecules.

Six compounds (2a11, 2a23, 2a17, 2a7, 2d11, and 2c7) were synthetized and submitted to the COX (ovine) Inhibitor Screening Assay Kit to examine its capacity to selectively inhibit COX-2 in vitro. The results found that, in corroboration with the docking analysis, all the compounds synthetized were more potent then celecoxib in inhibiting COX-2, also possessing a higher selectivity index.

In conclusion, the presented compounds can be further evaluated for in vivo models, based on the in silico and in vitro results, and could serve as hit molecules for the development of new COX-2 inhibitors.

Acknowledgements This study was financed in part by the Coordenação de Aperfeiçoamento de Pessoal de Nível Superior—Brasil (CAPES)—Finance Code 001, and, research support fund (FAP-UNIVALI).

Compliance with ethical standards

Conflict of interest The authors declare that they have no conflict of interest.

References

Baell JB, Holloway GA (2010) New substructure filters for removal of pan assay interference compounds (PAINS) from screening libraries and for their exclusion in bioassays. J Med Chem 53:2719–2740. https://doi.org/10.1021/jm901137j

Bandgar BP, Patil SA, Gacche RN, Korbad BL, Hote BS, Kinkar SN, Jalde SS (2010) Synthesis and biological evaluation of nitrogen-containing chalcones as possible anti-inflammatory and anti-oxidant agents. Bioorg Med Chem Lett 20:730–733. https://doi.org/10.1016/j.bmcl.2009.11.068

Berman HM (2000) The protein data bank. Nucleic Acids Res 28:235–242. https://doi.org/10.1093/nar/28.1.235

Brenk R, Schipani A, James D, Krasowski A, Gilbert IH, Frearson J, Wyatt PG (2008) Lessons learnt from assembling screening libraries for drug discovery for neglected diseases. ChemMedChem 3:435–444. https://doi.org/10.1002/cmdc.200700139

Daina A, Michielin O, Zoete V (2017) SwissADME: a free web tool to evaluate pharmacokinetics, drug-likeness and medicinal chemistry friendliness of small molecules. Sci Rep 7:1–13. https://doi.org/10.1038/srep42717

Daly AK, Rettie AE, Fowler DM, Miners JO (2018) Pharmacogenomics of CYP2C9: functional and clinical considerations. J Pers Med 8:1–31. https://doi.org/10.3390/jpm8010001

Danielson, ML, Hu, B, Shen, J, Desai, PV (2017) In silico ADME techniques used in early-phase drug discovery. In: Bhattachar, SN, Morrison, JS, Mudra, DR, Bender, DM (eds) Translating Molecules into Medicines. Springer Nature, Cham, Switzerland, p 81–117

de Pedro M, Baeza S, Escudero M-T, Dierssen-Sotos T, Gómez-Acebo I, Pollán M, Llorca J (2015) Effect of COX-2 inhibitors and other non-steroidal inflammatory drugs on breast cancer risk: a meta-analysis. Breast Cancer Res Treat 149:525–536. https://doi.org/10.1007/s10549-015-3267-9

Egan WJ, Merz KM, Baldwin JJ (2000) Prediction of drug absorption using multivariate statistics. J Med Chem 43:3867–3877. https://doi.org/10.1021/jm000292e

Enchev V, Mehandzhiyski AY (2017) Computational insight on the chalcone formation mechanism by the Claisen–Schmidt reaction. Int J Quantum Chem 117:1–8. https://doi.org/10.1002/qua.25365

Faria JV, Vegi PF, Miguita AGC, dos Santos MS, Boechat N, Bernardino AMR (2017) Recently reported biological activities of pyrazole compounds. Bioorganic Med Chem 25:5891–5903. https://doi.org/10.1016/j.bmc.2017.09.035

Gaonkar SL, Vignesh UN (2017) Synthesis and pharmacological properties of chalcones: a review. Res Chem Intermed 43:6043–6077. https://doi.org/10.1007/s11164-017-2977-5

Ghose AK, Viswanadhan VN, Wendoloski JJ (1999) A knowledge-based approach in designing combinatorial or medicinal chemistry libraries for drug discovery: a qualitative and quantitative characterization of known drug databases. J Comb Chem 1:55–68. https://doi.org/10.1021/cc9800071

Gomes, MN, Muratov, EN, Pereira, M, Peixoto, JC, Rosseto, LP, Cravo, PVL, Andrade, CH, Neves, BJ (2017) Chalcone derivatives: promising starting points for drug design. Molecules. https://doi.org/10.3390/molecules22081210

Hawkey C (1999) COX-2 inhibitors. Lancet 353:307–314. https://doi.org/10.1016/S0140-6736(98)12154-2

Karrouchi, K, Radi, S, Ramli, Y, Taoufik, J, Mabkhot, YN, Al-Aizari, FA, Ansar, M (2018) Synthesis and pharmacological activities of Pyrazole derivatives: a review, Molecules. https://doi.org/10.3390/molecules23010134

Khalaf N, Yuan C, Hamada T, Cao Y, Babic A, Morales-Oyarvide V, Kraft P, Ng K, Giovannucci E, Ogino S, Stampfer M, Cochrane BB, Manson JE, Clish CB, Chan AT, Fuchs CS, Wolpin BM (2018) Regular use of aspirin or non-aspirin nonsteroidal anti-inflammatory drugs is not associated with risk of incident pancreatic cancer in two large cohort studies. Gastroenterology 154:1380–1390.e5. https://doi.org/10.1053/j.gastro.2017.12.001

Khan MF, Alam MM, Verma G, Akhtar W, Akhter M, Shaquiquzzaman M (2016) The therapeutic voyage of pyrazole and its analogs: a review. Eur J Med Chem 120:170–201. https://doi.org/10.1016/j.ejmech.2016.04.077

Kim HS, Sharma A, Ren WX, Han J, Kim JS (2018) COX-2 Inhibition mediated anti-angiogenic activatable prodrug potentiates cancer therapy in preclinical models. Biomaterials 185:63–72. https://doi.org/10.1016/j.biomaterials.2018.09.006

Li J, Li D, Xu Y, Guo Z, Liu X, Yang H, Wu L, Wang L (2017) Design, synthesis, biological evaluation, and molecular docking of chalcone derivatives as anti-inflammatory agents. Bioorg Med Chem Lett 27:602–606. https://doi.org/10.1016/j.bmcl.2016.12.008

Li M, Zhao BX (2014) Progress of the synthesis of condensed pyrazole derivatives (from 2010 to mid-2013). Eur J Med Chem 85:311–340. https://doi.org/10.1016/j.ejmech.2014.07.102

Lipinski CA (2016) Rule of five in 2015 and beyond: target and ligand structural limitations, ligand chemistry structure and drug discovery project decisions. Adv Drug Deliv Rev 101:34–41. https://doi.org/10.1016/j.addr.2016.04.029

Lipinski CA, Lombardo F, Dominy BW, Feeney PJ (1997) Experimental and computational approaches to estimate solubility and permeability in drug discovery and development settings. Adv Drug Deliv Rev 23:3–25. https://doi.org/10.1016/S0169-409X(00)00129-0

Martin YC (2005) A bioavailability score. J Med Chem 48:3164–3170. https://doi.org/10.1021/jm0492002

Moroy G, Martiny VY, Vayer P, Villoutreix BO, Miteva MA (2012) Toward in silico structure-based ADMET prediction in drug discovery. Drug Discov Today 17:44–55. https://doi.org/10.1016/j.drudis.2011.10.023

Morris GM, Huey R, Lindstrom W, Sanner MF, Belew RK, Goodsell DS, Olson AJ (2009) AutoDock4 and AutoDockTools4: automated docking with selective receptor flexibility. J Comput Chem 30:2785–2791. https://doi.org/10.1002/jcc.21256

Muegge I, Heald SL, Brittelli D (2001) Simple selection criteria for drug-like chemical matter J Med Chem 44:1841–1846. https://doi.org/10.1021/jm015507e

Mukarram S, Bandgar BP, Shaikh RU, Ganapure SD, Chavan HV (2017) Synthesis of novel α,α-difluoro-β-hydroxycarbonyl pyrazole derivatives as antioxidant, anti-inflammatory and anticancer agents. Med Chem Res 26:262–273. https://doi.org/10.1007/s00044-016-1744-2

Özdemir A, Altıntop MD, Sever B, Gençer HK, Kapkaç HA, Atlı Ö, Baysal M (2017) A new series of pyrrole-based chalcones: synthesis and evaluation of antimicrobial activity, cytotoxicity, and genotoxicity. Molecules 22:2112. https://doi.org/10.3390/molecules22122112

Patrono C, Baigent C (2017) Coxibs, traditional NSAIDs, and cardiovascular safety post-PRECISION: what we thought we knew then and what we think we know now. Clin Pharmacol Ther 102:238–245. https://doi.org/10.1002/cpt.696

Pettersen EF, Goddard TD, Huang CC, Couch GS, Greenblatt DM, Meng EC, Ferrin TE (2004) UCSF Chimera: a visualization system for exploratory research and analysis. J Comput Chem 25:1605–1612. https://doi.org/10.1002/jcc.20084

Rayar A-M, Lagarde N, Ferroud C, Zagury J-F, Montes M, Sylla-Iyarreta Veitia M (2017) Update on COX-2 selective inhibitors: chemical classification, side effects and their use in cancers and neuronal diseases. Curr Top Med Chem 17:2935–2956. https://doi.org/10.2174/1568026617666170821124947

Richter L (2017) Topliss Batchwise Schemes reviewed in the era of open data reveal significant differences between enzymes and membrane receptors. J Chem Inf Model 57:2575–2583. https://doi.org/10.1021/acs.jcim.7b00195

Schmidt M, Lamberts M, Olsen AMS, Fosbøll E, Niessner A, Tamargo J, Rosano G, Agewall S, Kaski JC, Kjeldsen K, Lewis BS, Torp-Pedersen C (2016) Cardiovascular safety of non-aspirin non-steroidal anti-inflammatory drugs: Review and position paper by the working group for Cardiovascular Pharmacotherapy of the European Society of Cardiology. Eur Hear J Cardiovasc Pharmacother 2:108–118. https://doi.org/10.1093/ehjcvp/pvv054

Serhan CN, Savill J (2005) Resolution of inflammation: the beginning programs the end. Nat Immunol 6:1191–1197. https://doi.org/10.1038/ni1276

Shen FQ, Wang ZC, Wu SY, Ren SZ, Man RJ, Wang BZ, Zhu HL (2017) Synthesis of novel hybrids of pyrazole and coumarin as dual inhibitors of COX-2 and 5-LOX. Bioorganic Med Chem Lett 27:3653–3660. https://doi.org/10.1016/j.bmcl.2017.07.020

Singh P, Anand A, Kumar V (2014) Recent developments in biological activities of chalcones: a mini review. Eur J Med Chem 85:758–777. https://doi.org/10.1016/j.ejmech.2014.08.033

Sugimoto, MA, Sousa, LP, Pinho, V, Perretti, M, Teixeira, MM (2016) Resolution of inflammation: what controls its onset? Front Immunol. https://doi.org/10.3389/fimmu.2016.00160

Teague SJ, Davis AA, Leeson PD, Oprea T (1999) The design of leadlike combinatorial libraries. Angew Chemie Int Ed 38:3743–3748. https://doi.org/10.1002/(SICI)1521-3773(19991216)38:24<3743::AID-ANIE3743>3.0.CO;2-U

Tian S, Wang J, Li Y, Li D, Xu L, Hou T (2015) The application of in silico drug-likeness predictions in pharmaceutical research. Adv Drug Deliv Rev 86:2–10. https://doi.org/10.1016/j.addr.2015.01.009

Topliss JG (1972) Utilization of operational schemes for analog synthesis in drug design. J Med Chem 15:1006–1011. https://doi.org/10.1021/jm00280a002

Trott O, Olson AJ (2009) AutoDock Vina: improving the speed and accuracy of docking with a new scoring function, efficient optimization, and multithreading. J Comput Chem 8:NA–NA. https://doi.org/10.1002/jcc.21334

Umamaheswaran S, Dasari SK, Yang P, Lutgendorf SK, Sood AK (2018) Stress, inflammation, and eicosanoids: an emerging perspective. Cancer Metastasis Rev 37:203–211. https://doi.org/10.1007/s10555-018-9741-1

Veber DF, Johnson SR, Cheng HY, Smith BR, Ward KW, Kopple KD (2002) Molecular properties that influence the oral bioavailability of drug candidates. J Med Chem 45:2615–2623. https://doi.org/10.1021/jm020017n

Viveka S, Dinesha, Nagaraja GK, Shama P, Basavarajaswamy G, Rao KP, Yanjarappa Sreenivasa M (2018) One pot synthesis of thiazolo[2,3-b]dihydropyrimidinone possessing pyrazole moiety and evaluation of their anti-inflammatory and antimicrobial activities. Med Chem Res 27:171–185. https://doi.org/10.1007/s00044-017-2058-8

Wang JL, Limburg D, Graneto MJ, Springer J, Hamper JRB, Liao S, Pawlitz JL, Kurumbail RG, Maziasz T, Talley JJ, Kiefer JR, Carter J (2010) The novel benzopyran class of selective cyclooxygenase-2 inhibitors. Part 2: the second clinical candidate having a shorter and favorable human half-life. Bioorg Med Chem Lett 20:7159–7163. https://doi.org/10.1016/j.bmcl.2010.07.054

Wang Z, Sun H, Yao X, Li D, Xu L, Li Y, Tian S, Hou T (2016) Comprehensive evaluation of ten docking programs on a diverse set of protein–ligand complexes: the prediction accuracy of sampling power and scoring power. Phys Chem Chem Phys 18:12964–12975. https://doi.org/10.1039/C6CP01555G

van de Waterbeemd H, Gifford E (2003) ADMET in silico modelling: towards prediction paradise? Nat Rev Drug Discov 2:192–204. https://doi.org/10.1038/nrd1032

Zhuang C, Zhang W, Sheng C, Zhang W, Xing C, Miao Z (2017) Chalcone: a privileged structure in medicinal chemistry. Chem Rev 117:7762–7810. https://doi.org/10.1021/acs.chemrev.7b00020